Supporting information

SERS- and luminescence-active Au–Au–UCNP trimers for attomolar detection of two cancer biomarkers

Aihua Qu[1,2#], Xiaoling Wu [1,2#], Liguang Xu [1,2], Liqiang Liu[1,2], Wei Ma[1,2], Hua Kuang[1,2*], Chuanlai Xu[1,2*]

[1]*International Joint Research Laboratory for Biointerface and Biodetection, Jiangnan University, Wuxi, Jiangsu, 214122, PRC*

[2]*State Key Lab of Food Science and Technology, Jiangnan University, Wuxi, Jiangsu, 214122, PRC*

[*]Corresponding Authors: kuangh@jiangnan.edu.cn; xcl@jiangnan.edu.cn

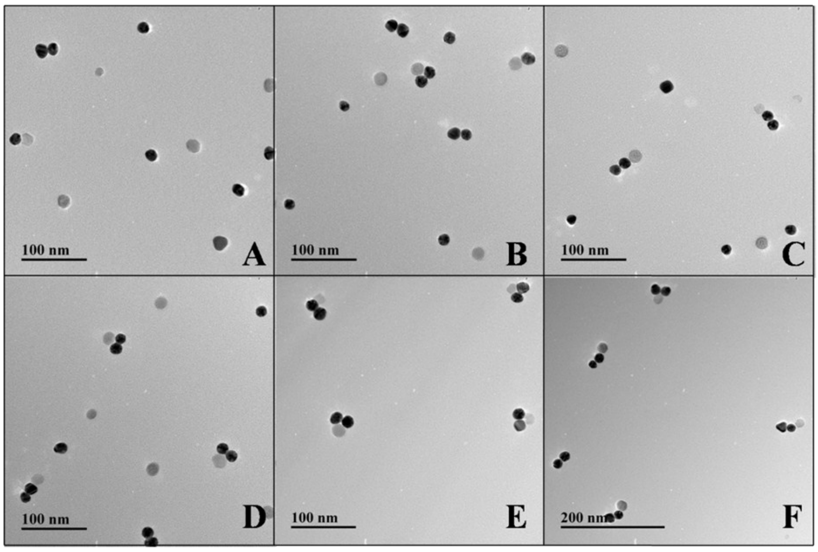

Fig. S1 TEM images of Au-Au-UCNP trimers assemblies with different time. (A) 0 h, (B) 2 h, (C) 4 h, (D) 8 h, (E) 12 h, (F) 16 h.

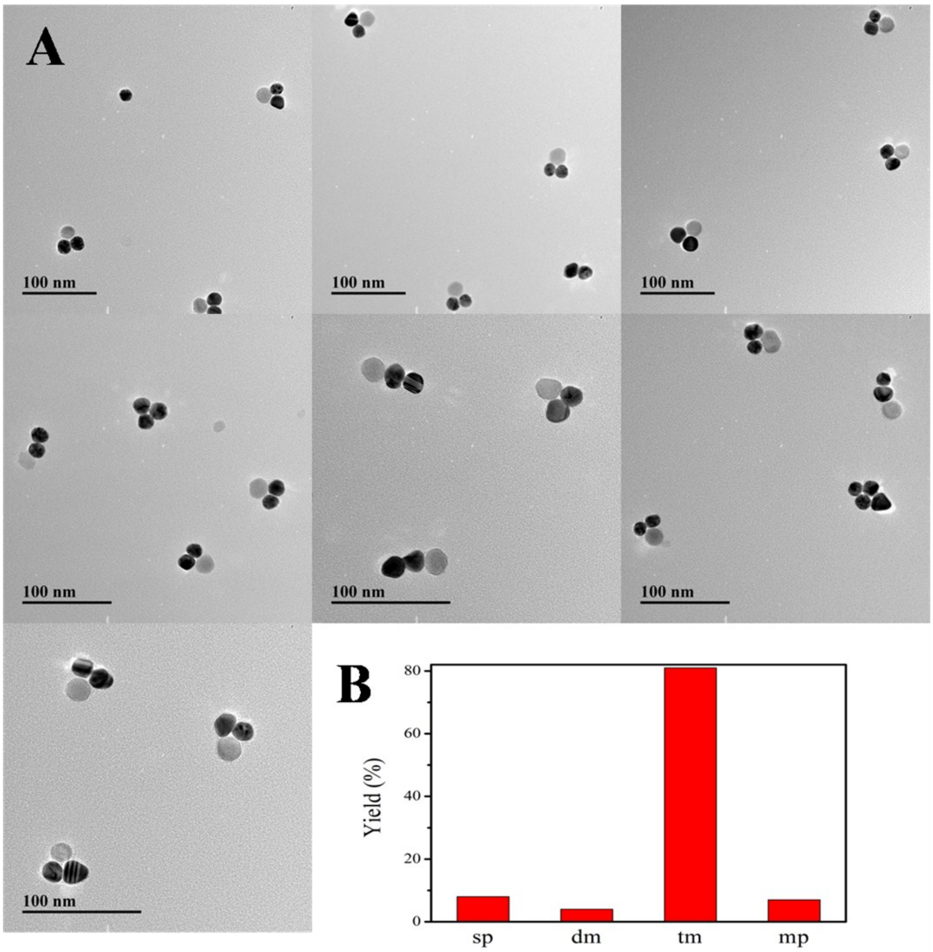

Figure. S2 (A) Representative TEM images of Au-Au-UCNP trimers in buffer. (B) Statistical analysis of different products in the reactions of trimers assembly. Notations “sp” , “dm” , “tm” , and “mp” stands for single-particles, dimers, Au-Au-UCNP trimers, and multiparticle assemblies (>3), respectively.

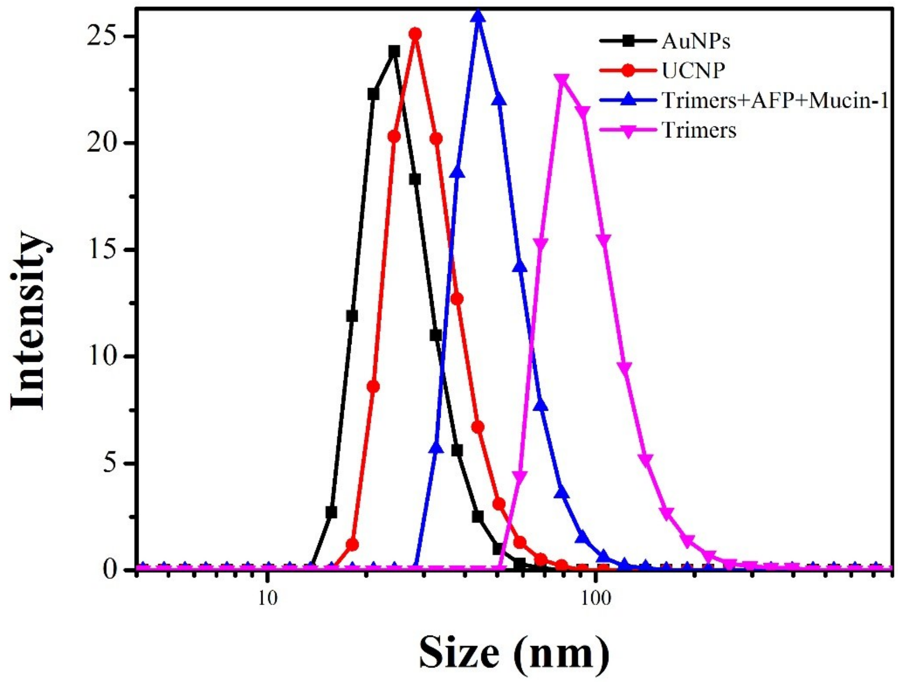

Fig. S3 DLS of Au NPs, UCNPs and Au-Au-UCNP trimers assemblies in the absence/presence of AFP and Mucin-1.

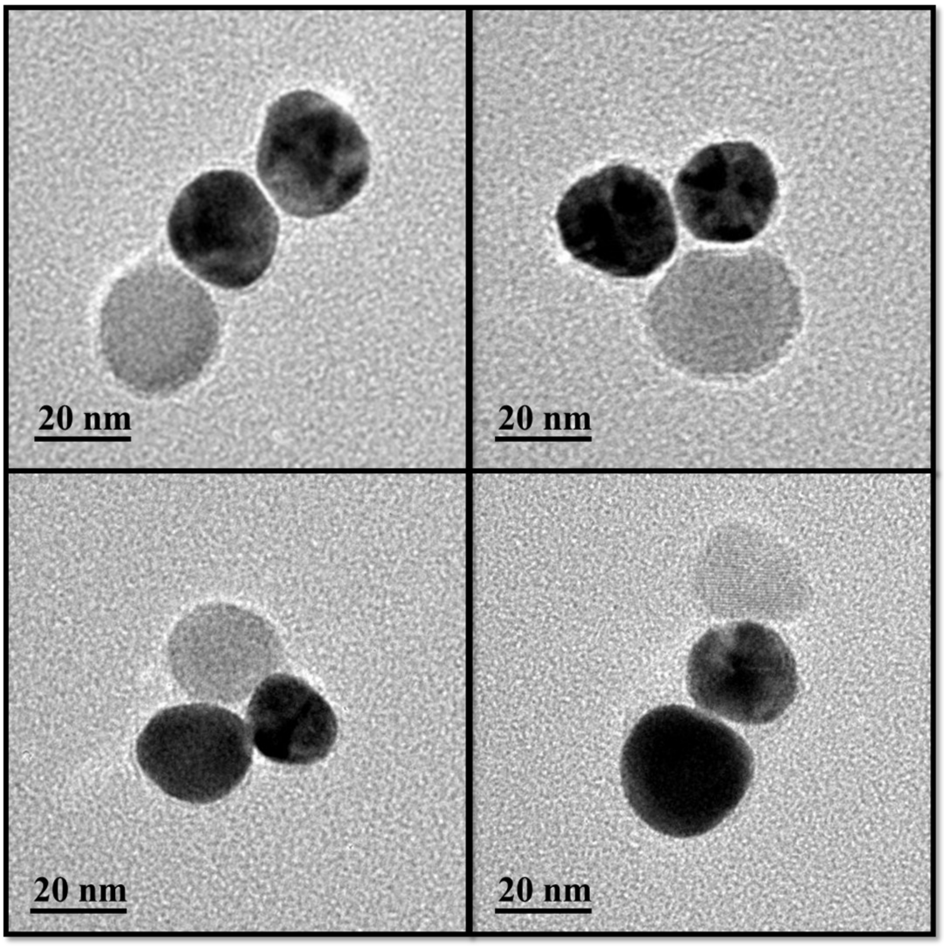

Fig. S4 Higher magnification TEM images of Au-Au-UCNP NPs trimers assemblies.

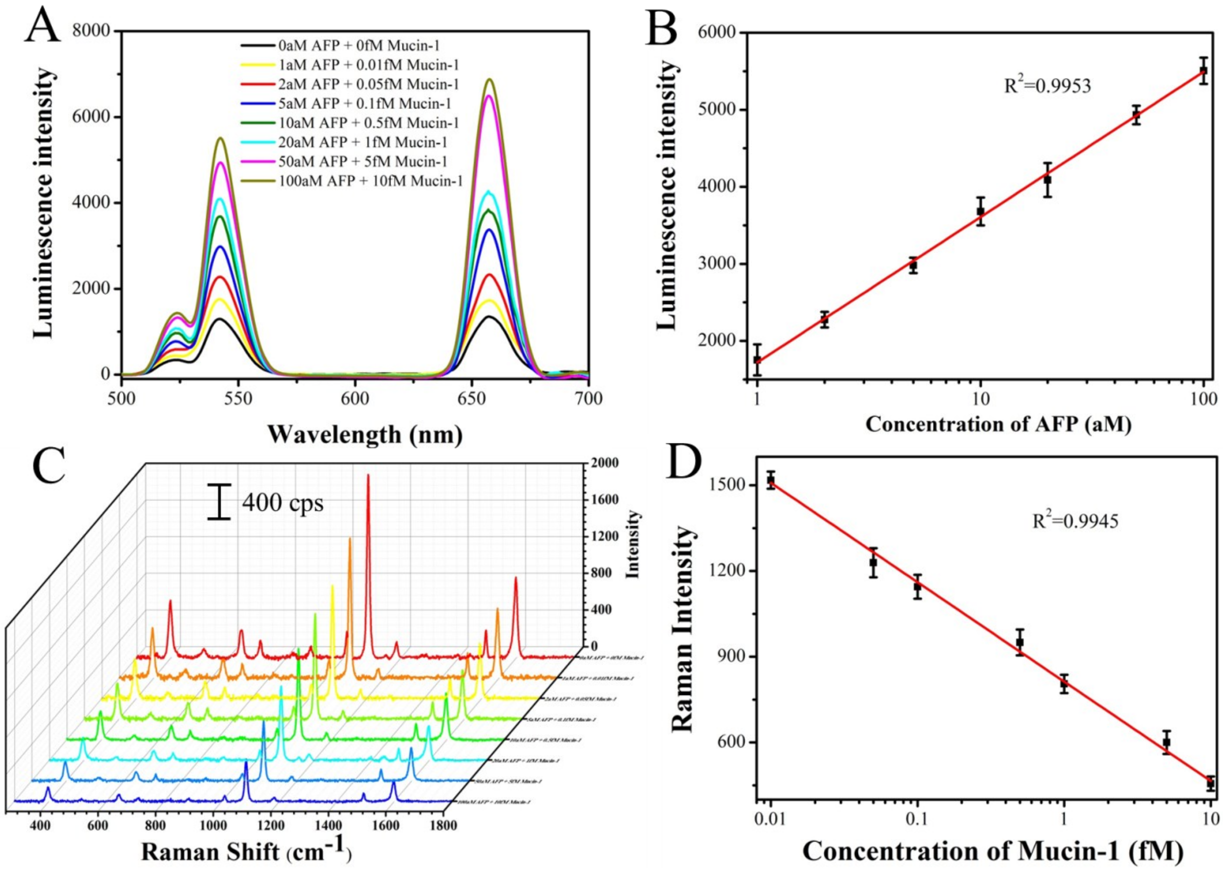

Fig. S5 AFP and Mucin-1 simultaneous detection based on luminescence and Raman with Au-Au-UCNP trimers. (A) luminescence spectra for different concentration of AFP and Mucin-1, (B) Standard curve for AFP detection with corresponding peak intensities at 542 nm, (C) Raman spectra for different concentration of AFP and Mucin-1, (D) Standard curve for Mucin-1 detection with corresponding peak intensities at 1084 cm^{-1}.

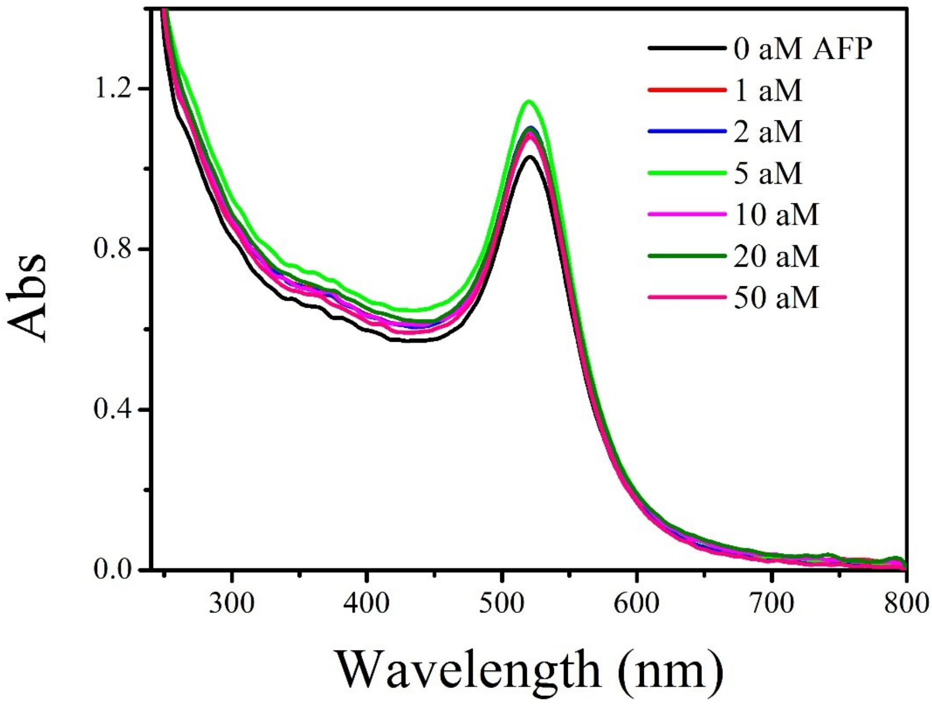

Fig. S6 The UV-Vis spectra for Au-Au-UCNP trimers assemblies with different concentration of AFP.

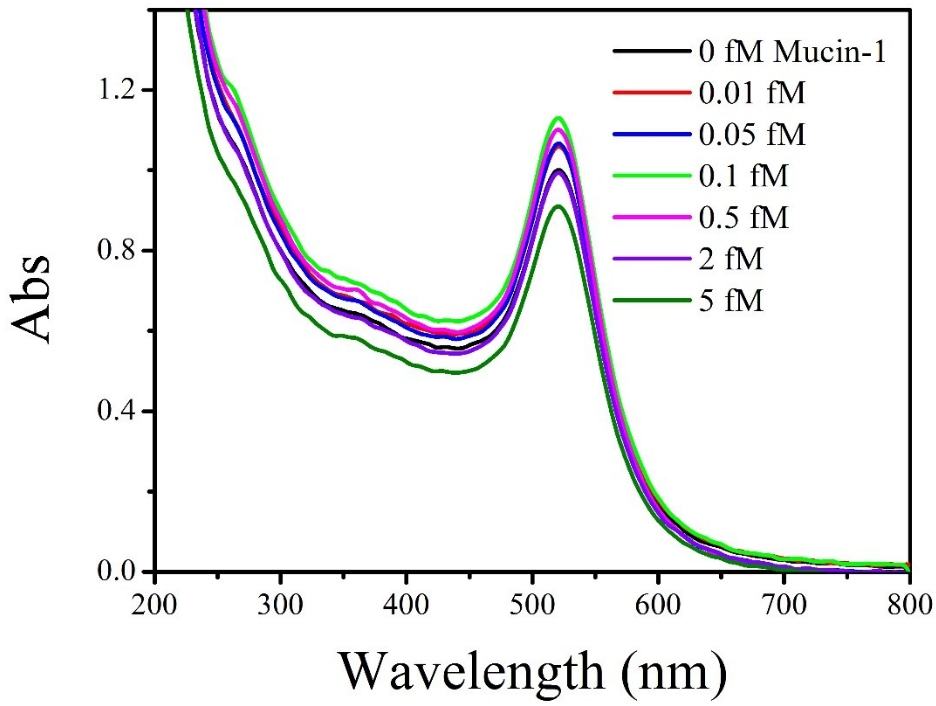

Fig. S7 The UV-Vis spectra for Au-Au-UCNP trimers assemblies with different concentrations of Mucin-1.

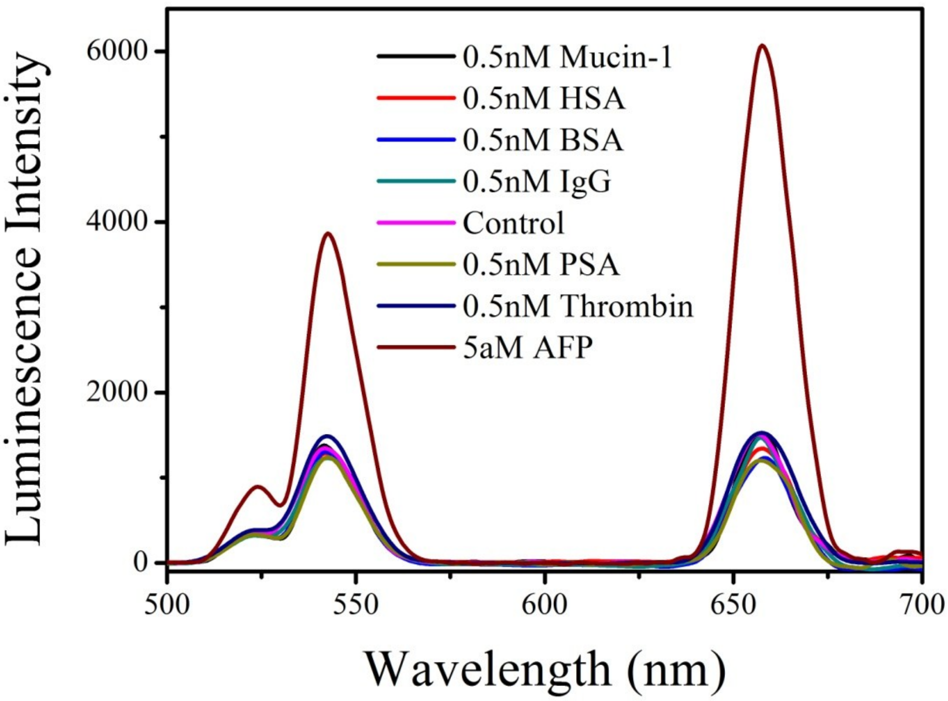

Fig. S8 Specificity of the luminescence active platform for the detection of AFP.

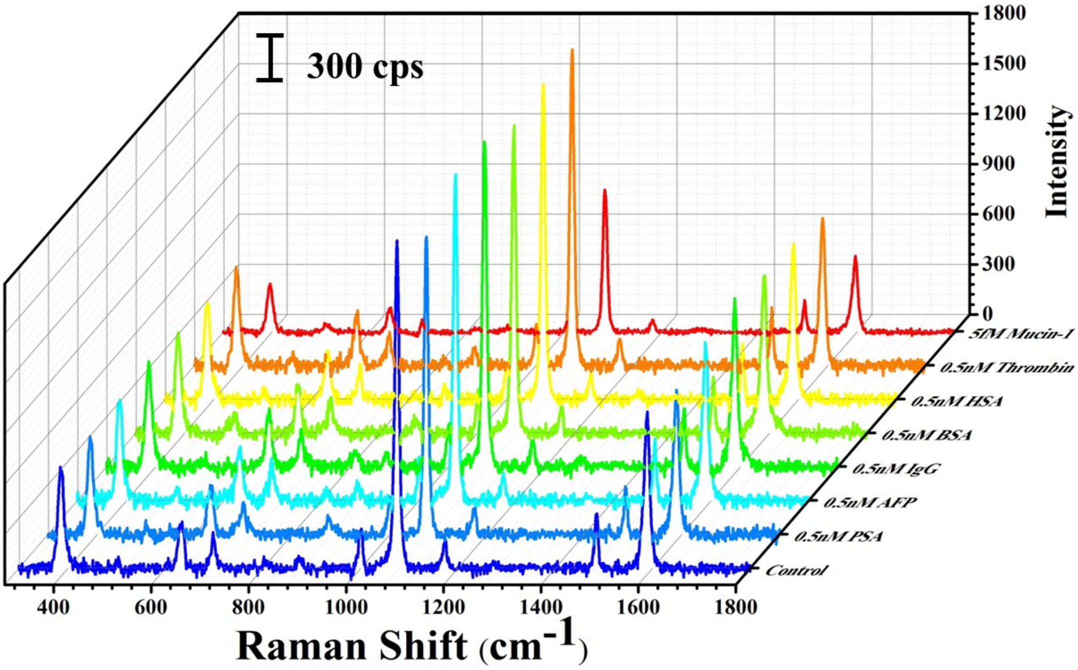

Fig. S9 Specificity of the SERS active platform for the detection of Mucin-1.

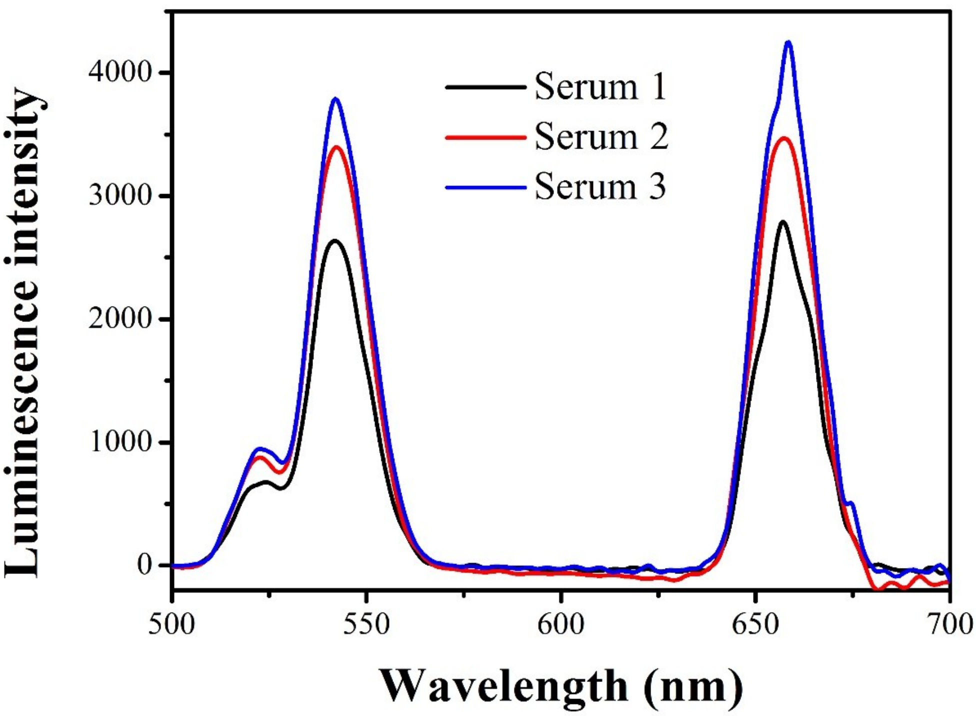

Fig. S10 Luminescence spectra of human serum samples diluted 10^5 times.

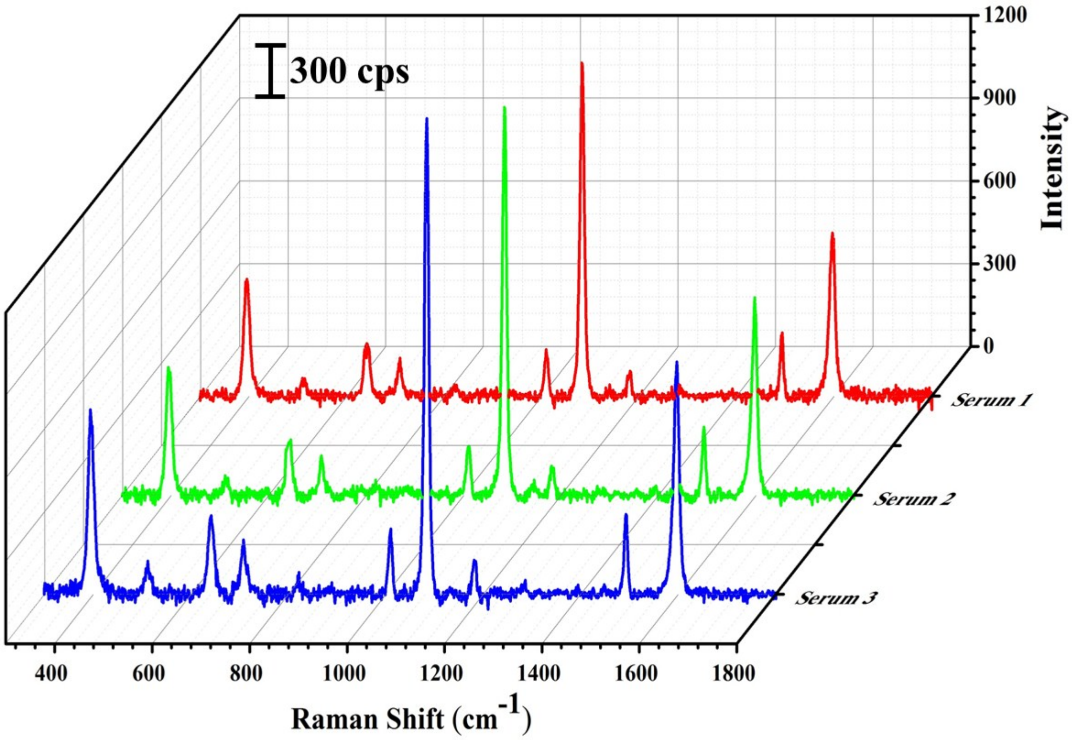

Fig. S11 Raman spectra of human serum samples diluted 10^5 times.

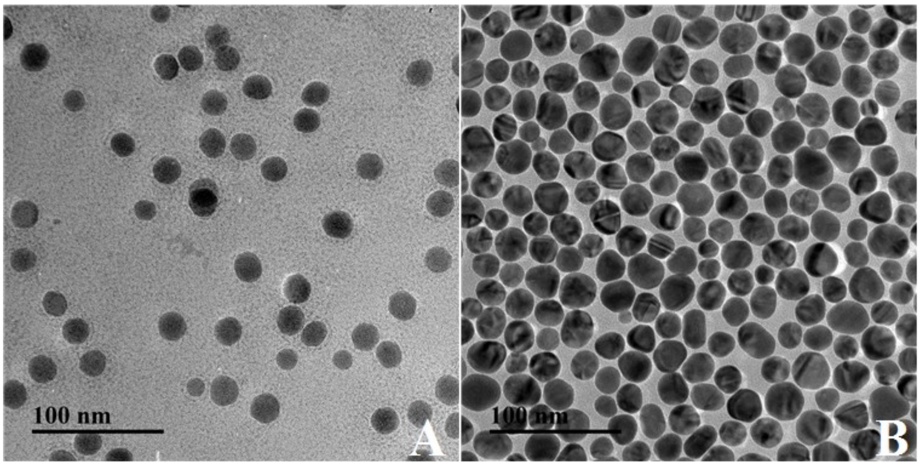

Fig. S12 (A) TEM of Upconversion nanoparticles. (B) TEM of Au nanoparticles.

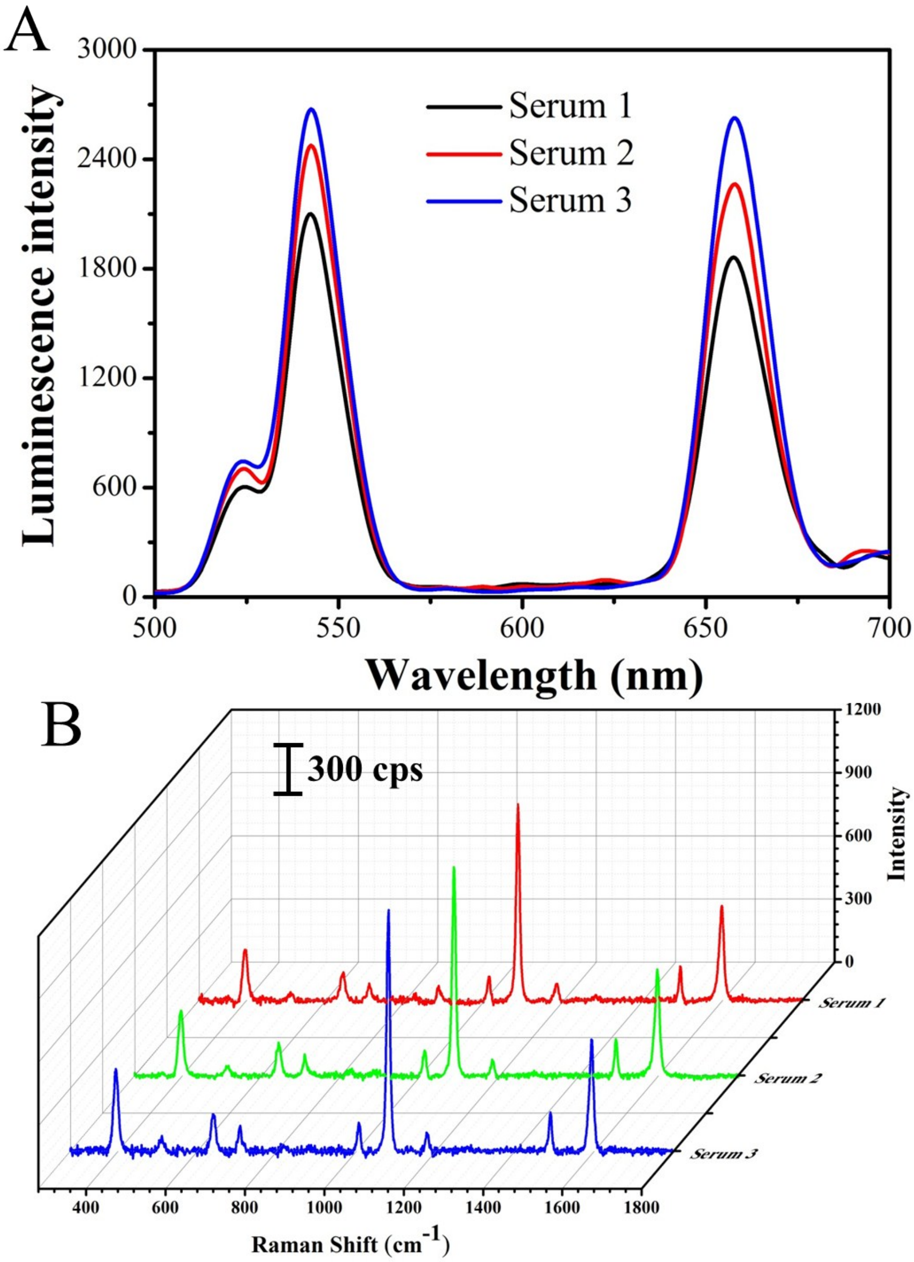

Fig. S13 (A) Luminescence spectra and (B) Raman spectra of human serum samples (AFP and Mucin-1 both coexist) diluted 10^5 times.

Table S1 DNA sequences for self-assembled Au-Au-UCNP trimers and applied in detection.

Types	Sequences
AFP-aptamer	5’-SH-GGCAGGAAGA CAAACAGGAC CGGGTTGTGT GGGGTTTTAAGAGCGTCGCC TGTGTGTGGT CTGTGGTGCT GT-3’
Mucin-1-aptamer	5’-GCAGTTGATCCTTTGGATAC CCTGG-SH-3’
Complementary	5’-GATCAACTGC ACAGCACCAC AGACC-SH-3’

Table S2 Practical analysis of AFP in human blood serum (n=3).

Serum samples	Original concentration (pM)	Diluted concentration (aM)	Detected concentration (aM)
1	12.9	1.29	1.31±0.21
2	17.1	1.71	1.73±0.32
3	19.8	1.98	2.01±0.24

Table S3 Practical analysis of Mucin-1 in human blood serum (n=3).

Serum samples	Original concentration (nM)	Diluted concentration (fM)	Detected concentration (fM)
1	6.1	0.61	0.62±0.13
2	3.3	0.33	0.36±0.32
3	1.6	0.16	0.14±0.24

Table S4 Practical analysis of AFP and Mucin-1 in human blood serum (n=3).

Serum samples	Original AFP concentration (pM)	Diluted AFP concentration (aM)	Detected AFP concentration (aM)
1	13.2	1.32	1.29±0.17
2	15.3	1.53	1.57±0.26
3	17.5	1.75	1.73±0.22
	Original Mucin-1 concentration (nM)	Diluted Mucin-1 concentration (fM)	Detected Mucin-1 concentration (fM)
1	5.8	0.58	0.55±0.21
2	4.3	0.43	0.47±0.34
3	2.1	0.21	0.18±0.18

Table S5 Other sensing systems of AFP detection.

Detection Method	Detection Limit	Detection Mode	Reference
Quantum-dot-based homogeneous time-resolved fluoroimmunoassay	0.4 ng/mL	singlet	[1]
Electrochemical immunosensor based on graphene nanocomposites	0.05 ng/mL	multiple	[2]
Gold Nanowire-Functionalized Carbon Nanotubes	0.01 ng/mL	singlet	[3]
Surface plasmon resonance imaging immunoassay	100 pg/mL	singlet	[4]
Homogeneous immunoassay and DNA hybridization assays using GNPs	714 fM	multiple	[5]
Photoelectrochemical Immunosensing	0.13 pg/mL	Singlet	[6]
Electrochemiluminescence biosensing	0.031 ng/mL	Singlet	[7]
Electrochemiluminescent immunosensor based on Graphene–Ruthenium(II) Composites	0.2 pg/mL	Singlet	[8]
Au@Ag nanorod-based colorimetric sensor	30 pg/mL	Singlet	[9]
Carbon Nanotubes Multifunctionalized by Rolling Circle Amplification	70 aM	double	[10]
SERS-active silver nanoparticle trimers	0.097 aM	Singlet	[11]

Table S6 Other sensing systems of Mucin-1 detection.

Detection Method	Detection Limit	Detection Mode	Reference
Electrochemiluminescence System Coupled with Target Recycling Amplification Strategy	2.8 fg/mL	double	[12]
SERS active bimetallic core-satellite nanostructure	4.3 aM	multiple	[13]
Electrochemical aptamer biosensor based on an enzyme–gold nanoparticle	2.2 nM	singlet	[14]
Carbon Nanospheres Featured Fluorescent Aptasensor	6.52 nmol/L	singlet	[15]
Impedimetric aptasensor based on gold nanoparticles	0.1 nM	singlet	[16]
Aptamer-based electrochemical Biosensor	50 nM	Singlet	[17]
SERS Encoded Silver Pyramids	9.2 aM	Multiple	[18]
Electrochemiluminescence immunosensor based on AuNPs@Fe_3O_4 nanocomposite	4.5 fg/mL	Singlet	[19]
Electrochemiluminescence Biosensor Based on Au-ITO Hybrid Bipolar Electrode	0.5 fM	Singlet	[20]

Reference

[1] M. J. Chen, Y. S. Wu, G. F. Lin, J. Y. Hou, M. Li, T. C. Liu, *Anal. Chim. Acta* 2012, **741**, 100-105.

[2] X. Chen, X. L. Jia, J. M. Han, J. Ma, Z. F. Ma, *Biosens. Bioelectron*. 2013, **50**, 356-361.

[3] H. Z. Cui, C. L. Hong, A. Ying, X. M. Yang, S. Q. Ren, *Acs Nano* 2013, **7**, 7805-7811.

[4] W. H. Hu, G. L. He, T. Chen, C. X. Guo, Z. S. Lu, J. N. Selvaraj, Y. Liu, C. M. Li, *Chem. Commun*. 2014, **50**, 2133-2135.

[5] C. Xie, F. Xu, X. Huang, C. Dong, J. Ren, *J. Am. Chem. Soc*. 2009, **131**, 12763-12770.

[6] Y. J. Li, M. J. Ma, J. J. Zhu, *Anal. Chem*. 2012, **84**, 10492-10499.

[7] S. L. Liu, J. X. Zhang, W. W. Tu, J. C. Bao, Z. H. Dai, *Nanoscale* 2014, **6**, 2419-2425.

[8] F. N. Xiao, M. Wang, F. B. Wang, X. H. Xia, *Small* 2014, **10**, 706-716.

[9] F. Zhang, J. Zhu, J.-J. Li, J.-W. Zhao, *J. Mater. Chem*. C 2015, **3**, 6035-6045.

[10] B. Zhao, J. Yan, D. F. Wang, Z. L. Ge, S. J. He, D. N. He, S. P. Song, C. H. Fan, *Small* 2013, **9**, 2595-2601.

[11] X. Wu, P. Fu, W. Ma, L. Xu, H. Kuang, C. Xu, *Rsc Adv*. 2015, **5**, 73395-73398.

[12] X. Jiang, H. Wang, H. Wang, R. Yuan, Y. Chai, *Anal. Chem*. 2016, **88**, 9243-9250.

[13] J. J. Feng, X. L. Wu, W. Ma, H. Kuang, L. G. Xu, C. L. Xu, *Chem. Commun*. 2015, **51**, 14761-14764.

[14] R. Hu, W. Wen, Q. L. Wang, H. Y. Xiong, X. H. Zhang, H. S. Gu, S. F. Wang, *Biosens. Bioelectron*. 2014, **53**, 384-389.

[15] C. Y. Li, Y. Meng, S. S. Wang, M. Qian, J. X. Wang, W. Y. Lu, R. Q. Huang, *Acs Nano* 2015, **9**, 12096-12103.

[16] X. Liu, Y. Qin, C. Y. Deng, J. Xiang, Y. J. Li, *Talanta* 2015, **132**, 150-154.

[17] F. Ma, C. Ho, A. K. H. Cheng, H. Z. Yu, *Electrochim. Acta* 2013, **110**, 139-145.

[18] L. G. Xu, W. J. Yan, W. Ma, H. Kuang, X. L. Wu, L. Q. Liu, Y. Zhao, L. B. Wang, C. L. Xu, *Adv. Mater*. 2015, **27**, 1706-1711.

[19] J. X. Wang, Y. Zhuo, Y. Zhou, R. Yuan, Y. Q. Chai, *Biosens. Bioelectron*. 2015, **71**, 407-413.

[20] M. S. Wu, D. J. Yuan, J. J. Xu, H. Y. Chen, *Anal. Chem*. 2013, **85**, 11960-11965.